Collapse of Highly Charged Polyelectrolytes Triggered by Attractive Dipole−Dipole and Correlation-Induced Electrostatic Interactions

A. G. Cherstvy*

IFF-2, Institut für Festköperforschung, Forschungszentrum Jülich, D-52425 Jülich, Germany, and Max-Planck-Institut für Physik komplexer Systeme, Nöthnitzer Straβe 38, D-01187 Dresden, Germany

Received: November 18, 2009; Revised Manuscript Received: February 20, 2010

In the first part of the paper, we study the collapse of flexible highly charged polyelectrolyte chains induced by attractive dipole−dipole interactions. The latter emerge due to the formation of dipoles between the chain monomers and counterions condensed on the polyelectrolyte from solution. Using the statistics of slightly perturbed Gaussian polymers, we obtain the scaling relations for the chain dimensions as a function of polyelectrolyte linear charge density in the limit of compacting chains. The results are in good agreement with the outcomes of recent molecular dynamics simulations of the collapse of flexible polyelectrolytes in the presence of explicit counterions. In the second part, we analyze the results of molecular dynamics simulations for the complex formation by two highly charged polyelectrolyte chains carrying opposite charges. We use the scaling arguments based on the picture of complexation of electrostatic blobs in order to rationalize the size of the complexes of two polyelectrolyte chains in the collapsed state. Similar scaling relation for the complex size was recently obtained in computer simulations of complexation of diblock polyampholytes and was described theoretically on the basis of similar electrostatic blob concepts. We also analyze the density of complexes formed and polyelectrolyte linear charge densities required for the onset onto the collapse as a function of interaction strength between the monomers. In both parts of the paper, we overview the scaling relationships obtained for similar systems with alternating charges from other theoretical approaches.

1. Introduction

The formation of complexes between polyelectrolytes (PEs) and oppositely charged objects is ubiquitous in chemistry and biophysics, including DNA wrapping in nucleosomes[1−4] and DNA compaction by multivalent counterions.[5−7] A simple picture of the collapse of a highly charged PE chain in the presence of neutralizing cations in solution is as follows. Weakly charged PEs with the Manning parameter $\xi = l_B/b = e_0^2/(\varepsilon k_B T b) \lesssim 1$ do not reveal a pronounced counterion condensation.[8−10] Here, b is the monomer−monomer distance, e_0 is the elementary charge, ε is the water dielectric constant, and l_B is the Bjerrum length in water, ≈7 Å at room temperature. Below the Manning threshold $\xi_M \approx 1$, the PE chains swell due to electrostatic (ES) repulsions between the monomers and their end-to-end distance grows with the number of monomers N faster than that for neutral polymers. For $\xi \gtrsim 1$, the condensation of counterions on the PE chain sets in and transient dipoles are formed between the chain monomers and cations condensed in their vicinity. This reduction of the PE charge impedes the growth of chain dimensions with the PE length. Also, possible attractive dipole−dipole (DD) interactions along the chain start to counteract the ES-induced PE swelling and they might in some cases lead to a collapse of highly charged PEs with condensed counterions.

Many theoretical investigations[11−22] and several computer simulation studies[22−27] are available in the literature on the interplay of ES repulsive and counterion-mediated attractive interactions along highly charged PE chains. Extensive simulations have in particular been performed on complexation of two oppositely charged PE[24] and polyampholyte chains[22] in solutions. A variety of scaling regimes for the PE chain dimensions as a function of the solvent quality and monomer−monomer interaction strength ξ have been suggested; see, e.g., ref 12. Still, some questions remain unanswered about the physical mechanism of the PE collapse, the dominant interactions triggering it, the structure of final complexes, the effect of added salt on the collapse transition, and scaling relations for the compact state of PE chains.

In this paper, we try to address some of these questions. We consider first the influence of ES and DD interactions on the conformational properties of flexible highly charged PE with condensed counterions. We start with the model of interaction-perturbed Gaussian polymers, obtain the results for PE dimensions treating the combination of ES and DD interactions, and then compare the outcomes with scaling predictions for PE collapse deduced from computer simulations. Then, we discuss a model of complex formation by two oppositely charged PE chains. Using the representation of complexing ES blobs, we suggest a scaling argument for the size of the globules formed at large interaction strengths, for the globule density, and PE length for the onset onto collapse. We investigate both weak and strong PE−PE complexation regimes. The scaling relations obtained for a single PE chain with condensed cations and derived for two complexing oppositely charged PEs are in good agreement with the results of recent computer simulations.

2. Collapse of a Single PE Chain with Condensed Cations

2.1. Model and Approximations. In this section, we study the collapse of a highly charged PE chain treated as a sequence of interconnected charged beads. The length of every monomer is fixed to $2a = l_B$, whereas the monomer point-like charge e varies. The chain contour length is $2a(N - 1)$ with $N \gg 1$, and

* E-mail: a.cherstvy@gmail.com.

10.1021/jp910960r © 2010 American Chemical Society
Published on Web 04/01/2010

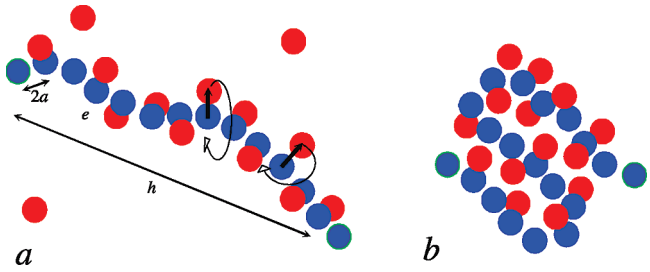

Figure 1. Schematic view of PE chains in (a) extended and (b) collapsed state, with dipoles fluctuating in the plane perpendicular to the local PE axis.

its end-to-end distance is denoted as h; see Figure 1a. We utilize a simple counterion condensation picture assuming that the PE starts to condense (monovalent) cations at $e > e_0$, when the PE linear charge density exceeds the threshold e_0/l_B. We set the fraction of cations condensed θ to be independent of the chain length, PE conformation, and extension, and to be equal to the Manning prediction for a thin straight PE at low concentration n_0 of 1:1 salt

$$\theta \approx 1 - 1/\xi \tag{1}$$

Note that several modifications of this law exist for flexible PEs in electrolyte solutions, where the degree of PE neutralization θ was shown to increase continuously with the PE linear charge density, with the counterion adsorption energy to the PE chain. Also, the PE ionization degree $1 - \theta$ was shown to decrease with increasing n_0, the monomer concentration, and chain flexibility.[28,29] Also note recent ref 53 where the effects of variable strength of counterion binding as a function of PE conformations, local dielectric permittivity, and PE ionization equilibrium on coil-to-globule transition of highly charged PE chains have been considered. Finite-length effects of PEs[30] and a depletion of counterion atmosphere near the chain ends[31] have also been elucidated.

In our model, the PE charge compensation fraction is set to

$$\theta(e) = (1 - e_0/e)\Theta(e/e_0 - 1) \tag{2}$$

where $\Theta(x)$ is the unit step function. For $e > e_0$, the DD interactions start to counteract the ES repulsions within the chain, Figure 1b. Above the Manning threshold, the PE charge density is renormalized so that the charge per monomer is reduced to $e(1 - \theta) = e_0$ and the charges on the dipoles formed are $\pm e\theta = \pm(e - e_0)$. This means that at $e > e_0$ all condensed cations participate in DD interactions and the PE linear charge density stays constant at e_0/l_B value. We assume no discrete values for the charge of condensed cations so that every PE monomer charge e can be reduced by counterions condensed down to e_0 per Bjerrum length. Then, the magnitude of dipoles formed by the chain monomer and nearest condensed cation is

$$p = 2a(e - e_0) \tag{3}$$

For instance, for the PE chain twice as charged as the Manning limit, we have $e = 2e_0$ and the dipole moment amounts to $p \approx 34$ D.

The dipoles are allowed in the model to rotate freely only perpendicular to the local PE axis, Figure 1a. This implies that the DD interaction energy is weaker than the thermal energy. We thus avoid treating a separate nontrivial problem of ordering and structure formation[13] by the dipoles on a PE chain for situations when dipoles interact with the energies $\gtrsim k_BT$. This free-rotation assumption implies that the dipoles are not subject to some constraints possibly imposed by the PE chemical structure. For instance, for the B-DNA with $\xi \approx 4.2$, the counterion-mediated forces are known to contribute to intermolecular interactions,[32−34] but the (condensed cation)−(phosphate group) dipoles are unlikely to rotate freely around the DNA axis because of the double-helical, grooved DNA structure.

As we assume a discrete nature of charges on the PE chain, the dipoles formed are rather attached to a particular chain monomer and not allowed to move along the PE backbone. The model with motions of condensed counterions allowed would be more relevant for PE chains that possess rather homogeneous charge distribution. We thus assume below a particular structure of a dipolar pair that might be relevant for some real PEs. We do not exclude that other ion pair models might be more appropriate for PEs with some nontrivial chemical structure, affecting the dipolar states to be formed. Also, the formation of permanent dipoles with particular spatial structure can occur along charged polymers with two types of charges.[21] Note that via fixing the PE charge compensation degree to the Manning value we avoid the treatment of equilibrium effects of salt ions and possible ion correlations on the chain.

For fluctuating dipoles, the average energy of DD interactions is attractive due to more favorable energy contributions originating from those conformations when fluctuating dipoles point in nearly opposite directions. This gives rise to polarization-induced average DD attraction that is implemented below as the driving force for the PE collapse. We do not consider here the ion−dipole forces[11] that, being averaged over all orientations of a dipole p fluctuating near a charge q, also give rise to an attractive potential $\langle E_{ion-dipole}(r)\rangle \approx -p^2q^2e^{-2\kappa r}/(6k_BT\varepsilon^2r^4)$.[35] This potential decays nearly exponentially with the charge−dipole separation, and it can be treated similarly to the average DD interactions, eq 4, using the scheme suggested below. In our model, however, the dipoles are allowed to rotate only perpendicular to the PE axis and thus ion−dipole interactions will not contribute to PE collapse upon increase in the PE charge density. In other words, the separation between charges of a dipoles and neighboring PE charge is nearly unaffected by dipole fluctuations allowed, while attractive forces between the neighboring fluctuating dipoles govern the PE collapse in the model.

We assume that ES and DD interactions perturb only weakly the Gaussian statistics of flexible PEs. Although this assumption clearly fails for dense PE globules, its applicability limits are not precisely defined. Also, the dielectric constant is set to $\varepsilon = 80$ everywhere and it is assumed for simplicity to be independent of the PE compaction state. The PE monomers interact via the common ES Debye−Hückel potential in weakly charged limit and by screened ES and screened average DD interactions above the Manning threshold. The Debye screening length in solution is $\lambda_D = 1/\kappa$. Below, we do not take into account the Donnan salt equilibrium, assuming the ionic conditions inside the PE coil/globule to be independent of chain compaction state. We thus neglect possible effects of accumulation of mobile counterions in a highly compacted state of a net-charged PE, that would be required to ensure the electroneutrality in the system; see ref 36.

2.2. Basic Equations. Average DD interaction energy between a dipole pair separated by distance r in electrolyte solution

can be approximated by

$$\langle E_{DD}(r)\rangle \approx -\frac{p^4 e^{-2\kappa r}}{4r^6\varepsilon^2 k_B T} \tag{4}$$

that is valid for $1/\kappa \gg a$. This energy is just 3/4 of the Keesom energy obtained through averaging of the DD interactions over all orientations of dipoles in space; see chapter 4.8 in ref 35. In eq 4, we consider for simplicity only the dominant exponential energy dependence on the DD separation r. The probability $w(h)$ to find the PE end-to-end distance in the interval h and $h + dh$ can be approximated by[37]

$$w(h)dh \approx h^2 \exp\left[-\frac{3h^2}{2\langle {h_0}^2\rangle} - \frac{\langle E_{DD}(h) + E_{ES}(h)\rangle}{k_B T} - \frac{vN^2}{2h^3}\right]dh \tag{5}$$

Here, $\langle {h_0}^2\rangle$ is the size of a neutral Gaussian chain, $\langle E_{DD}\rangle$ and $\langle E_{ES}\rangle$ are the average DD and ES interaction energies acting between all chain monomers, and the last term accounts for the excluded volume of monomers v.

The expression for $\langle E_{ES}\rangle$ within a weakly charged PE has been obtained long ago in refs 38 and 39

$$\langle E_{ES}(h)\rangle \approx k_B T l_B \frac{e^2 N^2}{{e_0}^2 h} \ln\left(1 + \frac{6h}{\kappa\langle {h_0}^2\rangle}\right) \tag{6}$$

It diverges at $\kappa \to 0$ because the sum of $1/r$ interactions along the PE chain does not converge. This expression was obtained summing the screened ES

$$E_{ES}(r) = k_B T l_B \left(\frac{e}{e_0}\right)^2 \frac{e^{-\kappa r}}{r} \tag{7}$$

interactions between the chain monomers and then averaging them over conformations of a Gaussian polymer.[39] Namely, the expression for the probability to find the distance r_k between two monomers that are k polymer segments apart along the chain has been utilized

$$W(r_k, k/N, h) = \sqrt{\frac{3}{2\pi\langle {h_0}^2\rangle(1 - k/N)}}\left(\frac{N}{k}\right)^{3/2} \times \frac{r}{h}\left\{\exp\left[-\frac{3(r - kh/N)^2}{2\langle {h_0}^2\rangle(1 - k/N)k/N}\right] - \exp\left[-\frac{3(r + kh/N)^2}{2\langle {h_0}^2\rangle(1 - k/N)k/N}\right]\right\} \tag{8}$$

For weakly charged PEs with ES interactions only, eq 5 predicts that PE dimensions grow linearly with the chain length, $h \propto N$. The chain extension becomes thus a constant fraction of PE length, and it was argued that in electrolyte solutions this method of PE ES energy calculation strongly overestimates the degree of chain expansion; see chapters 5.1.2 and 10.2 in ref 37. As a possible reason, it was suggested that molecular configurations with different ES energies are likely to have different statistical weights that might not be counted properly in this simple model. We still use below the ES energy (6) and implement the same statistical technique to calculate the average DD interaction energy $\langle E_{DD}(h)\rangle$ for a highly charged PE with condensed cations. We do so being interested mainly in scaling relations for the size of collapsing PE chains rather than in the absolute chain dimensions.

To average the DD interactions over the chain conformations, for long PEs $N \gg 1$, one can use the integration over the continuous variable $\zeta = k/N$ along the chain contour. As the screened DD interactions are very short ranged, only the nearest and probably next-nearest dipoles on the chain interact efficiently. Thus, one can extend the upper integration limit over from $\zeta = 1$ corresponding to the chain end to $\zeta = \infty$ to get

$$\langle E_{DD}(h)\rangle \approx N^2 \int_0^1 d\zeta \int_0^\infty dr E_{DD}(r) W(r, \zeta, h) \tag{9}$$

$$= -\frac{p^4 N^2}{4\varepsilon^2 h k_B T}\int_{a_1}^\infty dr \frac{e^{-2\kappa r}}{r^5}\left(e^{3rh/\langle {h_0}^2\rangle} - e^{-3rh/\langle {h_0}^2\rangle}\right)\int_0^\infty d\zeta \sqrt{\frac{3}{2\pi\langle {h_0}^2\rangle}}\zeta^{-3/2} e^{(3r^2/2\zeta\langle {h_0}^2\rangle) - (3h^2\zeta/2\langle {h_0}^2\rangle)} \tag{10}$$

We have put here as the lower integration limit over r the distance of the closest approach between the chain monomers $a_1 \sim 2a$. The integral over ζ is equal to $e^{-(3rh/\langle {h_0}^2\rangle)}/r$ and thus

$$\langle E_{DD}(h)\rangle = -\frac{p^4 N^2}{4\varepsilon^2 h k_B T}\int_{a_1}^\infty dr \frac{e^{-2\kappa r}}{r^6}\left(1 - e^{-6rh/\langle {h_0}^2\rangle}\right) \tag{11}$$

The integral over r gives

$$\langle E_{DD}(h)\rangle = -k_B T \frac{4N^2 {l_B}^2 a^4 e^4 \theta^4}{{e_0}^4 h} J(h) \tag{12}$$

where we define $J(h) = F(2\kappa) - F(2\kappa + 6h/\langle {h_0}^2\rangle)$, with $F(x) = (e^{-xa_1}/5)[(1/{a_1}^5) - (x/4{a_1}^4) + (x^2/12{a_1}^3) - (x^3/24{a_1}^2) + (x^4/24a_1)] + (x^5/120)Ei[-a_1 x]$ and $-Ei[-x] = \int_x^\infty (e^{-x'}/x')\, dx'$.

The PE extension is obtained via maximizing the probability density $\partial w(h)/\partial h = 0$ that gives the final transcendental equation for chain extension h

$$\frac{h^2}{\frac{2}{3}\langle {h_0}^2\rangle} = 1 + \frac{3vN^2}{4h^3} + 2{l_B}^2 N^2 a^4 \left(\frac{e\theta}{e_0}\right)^4\left[-\frac{J(h)}{h} + \frac{\partial J(h)}{\partial h}\right] - \frac{l_B N^2}{2h}\left(\frac{e(1 - \theta)}{e_0}\right)^2\left[\frac{6h/(\kappa\langle {h_0}^2\rangle}{1 + 6h/(\kappa\langle {h_0}^2\rangle)} - \ln\left(1 + \frac{6h}{\kappa\langle {h_0}^2\rangle}\right)\right] \tag{13}$$

In this equation, we have used eq 2 to calculate the prefactors for the ES and DD interactions. As $\langle E_{SS}(h)\rangle$ reveals a weaker dependence on the PE linear charge density than $\langle E_{DD}(h)\rangle$ does, the transition from the regime of PE expansion by ES repulsions to PE compression by average DD attractions is expected to take place as the PE linear charge density e/l_B grows.

2.3. Results. We have solved eq 13 first for an artificial fully neutralized PE chain with no ES interactions and with attractive DD interactions present at all e/e_0 values. As one could expect,

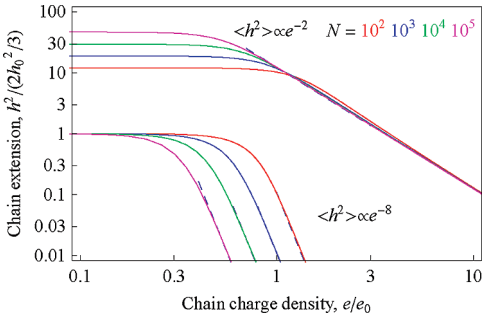

Figure 2. Dimensions of neutral chains with average DD attractions at all PE linear charge densities and with no ES repulsions. Excluded volume interactions are taken into account for the top set of curves, and they are neglected for the bottom set. The scaling asymptotes (14) and (15) are calculated for large PE charge densities and shown as dashed curves. Parameters: $a_1 = 2a$, $\kappa^{-1} = 1000$ Å, and monomer volume is $v = 4\pi a_1^3/3$.

as the PE charge density increases, the chain gradually collapses due to attractive DD interactions. For large e/e_0 values, the chain size in the compact state obeys the following scaling relations: in the absence of excluded volume interactions at $v = 0$, we get

$$h^2 \approx \left(\frac{4a_1^3 e_0^4}{3l_B^2 e^4}\right)^2 \propto e^{-8} \qquad (14)$$

and a weaker charge dependence is predicted for PEs with excluded volume effects, namely,

$$h^2 \approx \left(\frac{va_1^3 N^2 e_0^4}{l_B^2 e^4}\right)^{1/2} \propto e^{-2} \qquad (15)$$

The numerical solution of eq 13 for h shows that for shorter chains these scaling relations start to hold at larger PE linear chain charge densities, see Figure 2, because the attractive energy stored in the chain grows with the PE polymerization degree N.

For realistic PE chains, the counterion condensation starts at $e \sim e_0$, while for lower PE charge densities the polymer chains are extended by ES repulsions. After the DD forces switch on at $e/e_0 \gtrsim 1$, swollen PE coils start gradually forming more compact structures; see Figure 3. The collapse transition for such net-charged PE chains takes place at higher PE charge densities, as compared to artificial fully neutralized chains in Figure 2. Electrolyte solutions with very low salinity and with a Debye length of 1000 Å were implemented in Figures 2 and 3. It is important to note that PE charge densities for the onset onto collapse appear to be N-independent in this regime. We mention also that, due to ES-induced PE expansion, the excluded volume interactions have almost no effect on the dimensions of weakly charged PEs. Also, for the collapsed state of highly charged PEs, the PE dimensions obtained for the case with excluded volume interactions at $e/e_0 = 3 - 10$ resemble those for PEs without excluded volume effects; compare the two sets of curves in Figure 3. Only for the shortest chains treated, the excluded volume repulsion slightly swells the chains for very low and very high charge densities.

For larger κ values, we observe that weakly charged PE chains are considerably less extended because of better screening of ES repulsions by mobile ions in electrolyte. At small to moderate

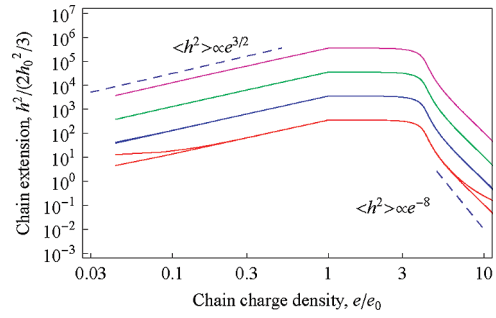

Figure 3. Chain dimensions of net-charged PEs, with Manning-like renormalized ES interactions and with DD interactions for $e/e_0 > 1$. Weakly charged PEs are expanded by ES repulsions, while highly charged PEs are collapsed by DD attractions. The two sets of curves are plotted for the case with and without excluded volume interactions, and they almost coincide for long chains. The deviations are only visible for the shortest chains, while for long PEs the excluded volume effects become pronounced at $e/e_0 \gtrsim 10$, the region not shown in the plot. Scaling relations for the chain dimensions are indicated as dashed curves. The color coding and parameters are the same as those in Figure 2, except the DD interactions are switched on here at the Manning threshold $e/e_0 = 1$.

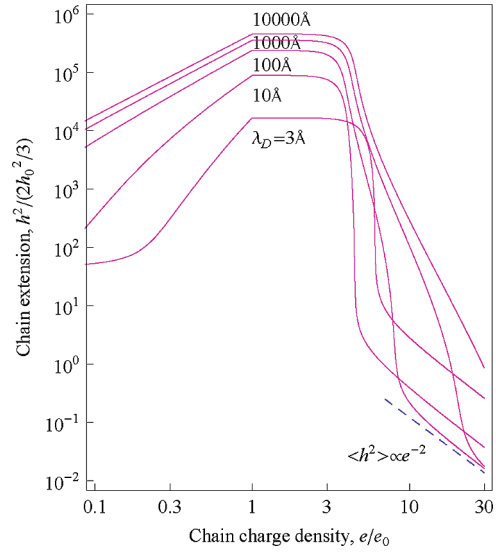

Figure 4. Chain dimensions for PEs with $N = 10^5$ monomers: as κ grows, weakly charged chains become less extended, while the size of globules formed by highly charged PEs reveals a nonmonotonous dependence on the salt concentration. The scaling asymptote (15) is shown as a dashed curve. The color coding and parameters used are the same as those in Figure 2.

salt concentrations, highly charged PEs exhibit more compact globules due to DD attractions and the transition to a compact state occurs sharper as a function of ξ; see Figure 4. Also, in the presence of excluded volume interactions, we observe that at larger κ values the chains start to follow the scaling relation (14) at lower PE linear charge densities. On the contrary, at high salt concentrations with Debye lengths $\lambda_D \gtrsim 30$ Å, the behavior of strongly charged PEs is reversed so that compacted chains start to swell substantially upon addition of salt up to ~1 M due to stronger screening of attractive DD interactions between the monomers. This critical screening length $\lambda_D \sim 30$ Å is pretty independent of the PE length N in the range of chain lengths considered. Note here that a similar effect of swelling for a compact state of polyampholyte chains upon addition of salt due to stronger screening of correlation-induced attractive interactions has been pointed out already in ref 42.

2.4. Comparison with Computer Simulations. Now, we analyze the results of molecular dynamics computer simulations

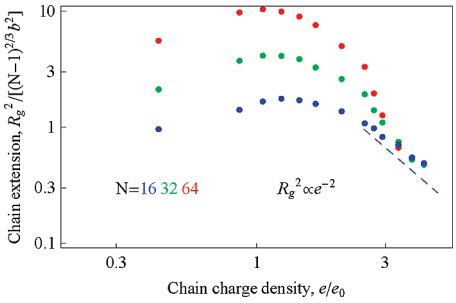

Figure 5. Rescaled gyration radius of highly charged PE chains with condensed cations. Dots are the results of computer simulations for different chain length N extracted from Figure 1 of ref 23. The scaling exponent for the compact state (eq 15) is the dashed curve.

of highly charged PE chains with their own condensed counterions performed in ref 23. This paper contains a detailed description of the simulation procedure as well as of intermonomer potentials and interaction parameters used. In particular, the simulations of highly charged PEs with increasing linear charge density at $\xi \gtrsim 3$ have revealed the formation of dense complexes and PE collapse was attributed to the formation and ordering of dipoles on strongly neutralized PEs. Namely, the condensed counterions were shown to neutralize almost 100% of the PE charge for highly charged $\xi \gg 1$ chains.[23] These nearly neutral collapsed chains assumed nearly globular shape even for the longest chains simulated, in contrast to the globule-necklace elongation transition known to occur for non-neutralized net-charged complexes of PE with their counterions; see the results of computer simulations and theoretical considerations presented in refs 40 and 41.

At large ξ values, the cations bind stronger to the PE backbone, forming ion pairs with the neighboring chain monomers. Simulations have revealed that the dipoles formed on neighboring chain monomers prefer to be oriented in nearly antiparallel directions. Doing so, the average energy of the DD interactions is negative due to a close proximity of charges of opposite signs and this DD attraction triggers a shrinkage of nearly net-neutral PE chains with condensed cations. It was shown in ref 23 that well below the Manning limit the chain's radius of gyration grows with chain length similarly to good-solvent conditions. Close to the counterion condensation threshold, the chain dimensions grow linearly with the number of monomers. Well above the Manning limit, a compact state of condensed PE is detected with the globule volume scaling linearly with chain length.

The simulation results obtained for the size of globules formed for different chain lengths nearly superimpose at large PE charge densities, which is indicative of the formation of a collapsed state. The PE globule dimensions at large ξ appear to follow the theoretical excluded-volume prediction eq 15, see Figure 5, where the simulation results for different chain lengths N and the theoretical scaling are shown.

Note that the simulations were performed at a fixed concentration of macroions and thus effectively at a finite, albeit small, concentration of counterions, preserving the electroneutrality in the system. Thus, the cations in the PE vicinity were subjected to ES potential created only by a finite chain fragment of the length $\sim\lambda_D$. This can be the reason why the onset on counterion condensation was found in simulations to be nearly independent of N; see Figure 1 of ref 23. At very low salt, however, the charge density required for the onset onto collapse for shorter PE chains is expected to be larger than that for long PEs. The reason being that long PEs facilitate the formation of dipoles by their higher attractive ES potential as compared to short PEs at the same linear charge density.

2.5. Other Models of PE Collapse. Let us mention the results of other theoretical models developed for the collapse of highly charged PE and polyampholyte chains into dense globules, when the collapse transition is governed at least partly by DD interactions between the monomers. For example, the second virial coefficient treatment of weak intersegmental averaged DD interactions along a highly charged PE chain with condensed counterions, $\langle E_{DD}(r)\rangle \propto -e^4/r^6$, has been presented in ref 11. As a result, the virial coefficient B grows quadratically with the PE interaction strength

$$B = 4\pi \int dr r^2 \left(1 - \exp\left[-\frac{\langle E_{DD}(r)\rangle}{k_B T}\right]\right) \propto \xi^2 \qquad (16)$$

and the size of the globule scales like

$$R \propto N^{1/3}|B|^{-1/3} \propto N^{1/3}\xi^{-2/3} \qquad (17)$$

The main disadvantage of this approach is that it fails to describe the behavior of PE chains with interactions of a longer range. In particular, the value of B diverges for Coulombic $1/r$ and for pure DD $1/r^3$ interactions between the chain monomers, making this virial coefficient approach inapplicable for quite realistic situations.

Other models for globular complexes in systems with "mixed" positive and negative charges utilize the ES Debye−Hückel polarization-induced attraction energy, $-\kappa^3 k_B TV/(12\pi)$, as a source of collapse of weakly oppositely charged PE chains and various polyampholytes.[42−47] For example, for neutral polyampholytes with randomly distributed charges, the competition of Debye−Hückel attraction energy and excluded-volume repulsions has been analyzed in ref 42 with the conclusion that without any salt at Θ-solvent conditions the size of the globular complex shrinks upon increase of ξ as $R \propto N^{1/3}\xi^{-1/3}$, while in good solvent conditions the two-body repulsion of monomers counteracting the ES charge-correlation attraction gives rise to $R \propto N^{1/3}\xi^{-2/3}$ scaling.

3. Complex Formation by Two Oppositely Charged PE Chains

3.1. Weak ES Association: Simulation Results. In this section, we discuss the scaling relations governing the collapse behavior of two oppositely charged PE chains that can also be influenced by attractive DD interactions. Recently, the complex formation between two[24] and several[48−51] oppositely charged PEs has been investigated by computer simulations. In particular, extensive molecular dynamics simulations have shown[24] that two oppositely charged PE chains of the same length and charge density, without any counterions, in salt-free solution align via forming nearly helical structures due to DD interactions at moderate PE charge densities of $\xi \sim 1-3$. The dipoles are formed by the neighboring contacting monomers of the paired PE chains. Similarly to a single PE with condensed cations, the dipoles prefer to point in opposite directions, that would result in a zigzag conformation of charges along this structure of two plied PEs. The chain connectivity and bonding potentails between the monomers however disfavor such a zigzag charge arrangement. As a result, quasi-helical structures of two PE chains emerge at equilibrium and their gyration radius initially grows as a function of interaction strength ξ. For larger $\xi \propto e^2$

Figure 6. Snapshots of the dynamics of collapse transition of two oppositely charged PE chains at $\xi = 8$, as obtained by molecular dynamics simulations. The graph is taken from Figure 8 of ref 24. Copyright 2002 APS.

values, these quasi-helical structures form "superhelices" collapsing onto themselves due to attractive DD-like interactions, the size of complexes decreases, and eventually the chains form nearly spherical globules. Figure 6 shows the dynamics of this complexation process.

Within a wide range of interaction strengths, for $0.1 \lesssim \xi \lesssim 20$, the size of these globules R_g and their monomer density ρ were shown in simulations to scale like[24]

$$R_g \propto N^{1/3}\xi^{-1/6}, \qquad \rho \propto \xi^{2/5} \tag{18}$$

It is important to mention that scaling relation (18) for interaction-strength dependence obtained for two PEs $R_g \propto e^{-1/3}$ is much weaker than for a single highly charged PE with the condensed counterions; see Figure 5. It is also much weaker than the scalings suggested for the complex formation in systems with alternating charges, where the relation $R \propto N^{1/3}e^{-4/3}$ is typically predicted. This might be indicative of different complexation mechanisms or some effects of the chain connectivity that suppress the outcomes of interactions responsible for the complex formation.

Contrary to a single PE chain with condensed cations, where the counterion condensation and the PE complexation start at $\xi \gtrsim 1$ and both phenomena are largely independent of the chain length,[23] the onset on complexation of two oppositely charged PEs is strongly chain-length-dependent.[24] Namely, longer chains enter the collapse regime at the PE linear charge densities that produce Manning parameters that are 10−100 times lower than the $\xi = 1$ threshold. Longer chains start to follow the scaling relation (18) for R_g at smaller ξ values because the total attractive interaction energy in the system is likely to grow as $\propto N^2$ for the coiled PE chains.[24] For even stronger interactions, at $\xi \gtrsim 20-50$, nearly close-packed structures of the chain monomers were observed in simulations, with even weaker complex size dependence on ξ. In this regime, the complex dimensions are governed by the excluded volume of the monomers that prefer to surround themselves in the complexes by monomers of opposite charge at these extreme compactions.

3.2. Polymer Properties and the Model of ES Blobs. The weak $R_g(\xi)$ dependence (18) observed for the complexes of two oppositely charged PEs has recently been reproduced by extensive molecular dynamics computer simulations for a quite similar system of collapsing diblock polyampholyte molecules consisting of two connected oppositely charged PE segments otherwise identical.[22] Namely, it was shown that in good solvent at moderate interaction strengths the complex gyration radius and its density scale like

$$R_g \propto \xi^{-0.18}, \qquad \rho \propto \xi^{0.54} \tag{19}$$

The coil-to-globule transition observed for polyampholytes was triggered by fluctuation-induced ES attractive interactions between oppositely charged parts of the molecular chain.

The successful scaling approach has been suggested in ref 22 for description of simulation data for the globule size at moderate ξ values. It is based on fluctuation-induced ES association of charges and utilizes the picture of ES blobs and further association of blobs into larger assemblies. According to the common procedure, the interaction of charges within one ES blob is considered to be smaller than the thermal energy and polymer conformations are almost unperturbed by ES interactions. The size of the ES blob R_b and the number of monomers in the blob N_b are obtained from the fact that the energy stored in the blob is $\sim k_BT$. That gives $R_b \propto b(\xi f^2/b)^{-\nu/(2-\nu)}$ and $N_b \propto (\xi f^2/b)^{-1/(2-\nu)}$. Here, $\nu \approx 0.588$ is the excluded volume exponent for the polymer chain, f is the fraction of charged monomers in the chain (at $f = 1$, all monomers are charged), and b is the monomer length. For long polymers consisting of many blobs, $N \gg N_b$, the fluctuation-induced interactions between ES blobs with the energy of $\sim k_BT$ result in the formation of relatively compact, globular structures of blobs. The ES blobs prefer to be surrounded by the oppositely charged blobs, similarly to positive−negative charge clustering in every blob itself. The radius of these aggregates of ES blobs R_g and the monomer density in them ρ scale like[22]

$$R_g \propto R_b(N/N_b)^{1/3} \propto \left(\frac{\xi f^2 N^2}{R_{g0}}\right)^{(1-3\nu)/3(2-\nu)}, \qquad \rho \propto N_b/{R_b}^3 \propto b^{-3}\left(\frac{\xi f^2}{b}\right)^{(3\nu-1)/(2-\nu)} \tag{20}$$

Here, $R_{g0} \propto bN^{\nu}$ is the gyration radius of an unperturbed polymer chain. For $\nu = 0.588$, the scaling exponents in eq 19 follow from the general consideration in eq 20. Note that, similarly to computer simulations of two PE chains[24] performed in the absence of salt, this ES blob theory does not account for the Debye exponential screening of charges by mobile electrolyte ions.

3.3. Comparison with Computer Simulations. The comparison of theoretical scaling (18) with the outcomes of simulation data for the globule formation by two oppositely charged PE chains is presented in Figure 7. Numerical results for the PE chains of $N = 20$, 40, 80, and 160 monomers are shown in the figure, with the gyration radius plotted after rescaling the simulation data with $R_g \sim N^{1/3}$, the typical dependence for dense states of a polymer. Although the original empirical exponent $R_g \propto \xi^{-1/6}$ [27] seems to fit the data of ref 24 slightly better and in a wider range of PE charge densities, the

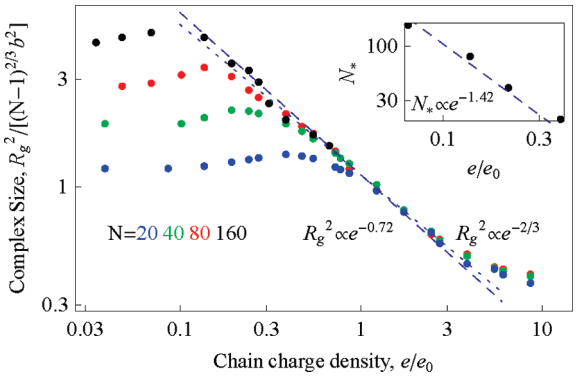

Figure 7. Rescaled gyration radius of the complexes of two oppositely charged PE chains of different length N. The data are extracted from Figure 1 of ref 24. Copyright 2002 APS. The PE charge density for the onset onto collapse for the corresponding chain lengths N^* is presented in the inset. Scaling relations (19) and (21) are shown as dashed lines, while scaling relation (18) is the dotted curve. The simulation data for PEs with different numbers of monomers N are color coded.

theoretical expectation $R_g \propto \xi^{-0.18}$ derived for the assembly of ES blobs[22] also exhibits excellent agreement with simulation data.

One origin of discrepancy can probably be the finite and relatively short chain lengths used in the simulations of ref 24. Figure 7 indeed shows that for longer chains the complex extensions obey the scaling law predicted in a larger range of the chain charge densities. Also, the theory of complexation of ES blobs does not account directly for the chain connectivity, allowing thus for any hypothetical, most energetically profitable arrangement of electric charges in the blobs. The latter being the complexes with the charges of one sign surrounded prevalently by the charges of the opposite sign; see the next subsection. This might be the reason for a slightly stronger dependence $R_g(\xi)$ predicted from the blob assembly picture than $R_g \propto \xi^{-1/6}$ observed in simulations.[24]

Also, related to this "charge freedom" issue, in computer simulations of polyampholyte chains,[22] the fraction of charged monomers was typically 1/8 or 1/4 of the total number of monomers, allowing thus an energetic adjustment of charges to their neighboring "favorite" charges, due to a larger number of intermediate neutral monomers. For the complexation of oppositely charged PEs,[24] all monomers were charged and thus in the dense PE−PE complexes every charge had unavoidably at least two charges of the same sign as first neighbors. This might be a reason for a slightly stronger dependence of the complex size upon ξ observed for the complexation of adjustable polyampholytes and predicted by the ES blob theory,[22] as compared to a more restricted system of two complexing oppositely charged PE chains.[24]

The theory of complexation of ES blobs also suggests a relationship between the chain charge density and the chain length for the onset onto the PE−PE collapse transition. Namely, at this point, the size of the ES blob is of the same order as the size of the whole chain assembly, $R_g \propto R_{g0}$. In Θ-solvent conditions, it gives the following dependence for the minimal chain length required to trigger the collapse as a function of ES interaction strength[22]

$$N_* \propto \xi^{-1/(2-\nu)} \propto e^{-1.42} \tag{21}$$

This prediction reveals a good agreement with the simulation results,[24] as shown in the inset of Figure 7. For this graph, the maximum of the gyration radius of the complexed PE chains as extracted from simulations, that is, the point of extension-to-compression turnover of the complex, was used as the onset onto the coil−globule transition in the system.

Note here that, although the ES blob model does predict the weak scaling exponent (18), it does not provide a clear hint why, as the strength of ES interactions along the chain grows, the size of a single highly charged PE chain with condensed counterions[23] shrinks in much more pronounced fashion than the dimensions of two complexed oppositely charged PEs,[24] despite the fact that both systems contain a nearly neutral assembly of interacting positively and negatively charged monomers. One possible reason is that the freedom of dipoles formed along two complexed PE chains is strongly hindered as compared to freely rotating dipoles on a single PE with condensed cations.

3.4. Strong ES Association: Ionic Crystals. As mentioned above, at even stronger interaction strengths, at $\xi \gtrsim 20$, the complex size reveals even weaker dependence on the chain charge density; see Figure 7. This regime is dominated by excluded volume interaction of monomers that prevents further compaction of complexes. The picture of ionic association and formation of multiplets can be implemented in this limit to treat the collapse in systems with alternating charges; see ref 22. Namely, for a similar system of polyampholytes at large interaction strengths, the cascade of multiplets of increasing order (dipole, quadrupoles, etc.) was shown to emerge with increasing interaction strength, which was suggested to govern the collapse transition in the system. In this limit, the charge−charge interaction energy exceeds k_BT dramatically and it can easily overcome the entropic penalty of confinement of a polymer chain into a proper conformation that minimizes the ES energy via forming charge configurations reminiscent of those in ionic crystals; see Figure 1b. In such a situation, not only ES and averaged DD interactions but also other types of interactions like ion−dipole and direct DD contacts in complexes can contribute to the collapse properties and scaling relations for the complex size $R(\xi)$.

Below, we mimic the complexes of oppositely charged PEs at large ξ values as a dense assembly of disconnected positively and negatively charged monomers with different kinds of possible attractive interactions acting between them (ES, ion−dipole, DD, and average DD). Because a short-ranged r^{-12} Lennard-Jones repulsive potential was used in simulations to prevent the complete chain collapse,[24] the energy per monomer in a dense globule can be written in this limit as a sum of attractive and repulsive contributions

$$E(r) \sim -e^{\alpha}/r^{\beta} + 1/r^{12} \tag{22}$$

where r is the separation between neighboring monomers. Here, $\alpha = 2$ and $\beta = 1$ for ES, $\alpha = 2$ and $\beta = 2$ for ion−dipole, $\alpha = 2$ and $\beta = 3$ for DD, and $\alpha = 4$ and $\beta = 6$ for averaged DD interactions. The optimal r_0 value follows from the energy minimum over r. As for dense globules the density scales as $\rho \propto r_0^{-3}$, we get

$$\rho \propto e^{3\alpha/(12-\beta)} \tag{23}$$

The scaling for the gyration radius of globules is $R \propto N^{1/3}\rho^{-1/3} \propto N^{1/3}e^{-\alpha/(12-\beta)}$. This gives rise to the following scaling relations

$$R_{ES} \propto e^{-2/11}, \qquad R_{ion-dipole} \propto e^{-2/10}, \qquad R_{DD} \propto e^{-2/9}, \qquad R_{\langle DD \rangle} \propto e^{-2/3} \tag{24}$$

for the corresponding types of attractive interactions, where e is the monomer charge.

The average DD interactions are unlikely to be realized in this regime due to closely packed monomers and thus prohibited fluctuations of charges. Other scalings presented above are weaker than the $R \propto e^{-1/3}$ dependence extracted from simulations of PEs at intermediate interaction strengths, Figure 7. The ion crystal formation counteracted by the finite-size potential between the monomers can thus be the physical rationale for a considerably weaker $R_g(\xi)$ dependence observed at large PE interaction strengths in simulations; see the $\xi \gtrsim 20$ domain in Figure 7. Note also that, as the strength of corresponding interactions varies with r in a different manner, the range of the globule densities where scaling relations (24) for $R(\xi)$ might hold will change for each type of complexation force considered.

4. Discussion

After this paper was submitted, we became aware of two very closely related studies of the PE collapse.

4.1. Single PE Chain. In the first very recent study, the conformational behavior of highly charged poly-zwitterionic polymers with the charges of both signs on every chain monomer has been considered theoretically using the variational approach.[21] Screened intrinsic DD as well as induced ion−dipole and induced DD interactions were considered in the model, using the assumption of freely rotating dipoles on the chain. This gave rise to two attractive contributions—the average ion−dipole and average DD interactions—and their interplay with the screened repulsive ES interactions of noncompensated charges was elucidated. Attractive DD interactions were shown to result in a shrinkage of the chain at low salt concentrations, when the attraction energy dominates over the entropy reduction of collapsing chain. Upon increase in salinity, however, in the DD-attraction dominated regime, the chains were shown to swell due to a stronger screening of attractive interactions. This chain swelling and increase in the radius of gyration was attributed to a better solubility of zwitterionic polymers at higher salt amounts, that is indeed observed experimentally. This salt-induced solubilization behavior was called the anti-PE effect, being opposite to the effect typically observed for PEs, where upon addition of salt the strength of ES repulsions along the PE chain is reduced and the PE solubility is diminished because of smaller chain sizes.

The main difference between the present study and results presented in ref 21 is that the latter considers the free rotation of dipoles on the chains that necessitates the consideration of both average ion−dipole and DD interactions. The model suggested in section 2 is, on the other hand, limited to rotations of dipoles only perpendicular to the PE axis, and thus, solely the averaged DD attractive term is to be taken into account. Note also that, despite much more elaborate treatment of counterion condensation effects and attractive ion−dipole and DD interactions in ref 21, the underlying physical assumption of both approaches about the free rotation of dipoles formed on PE chain is pretty similar. These dipoles' fluctuations are totally unrestricted in ref 21, and they are limited to the plane perpendicular to the PE axis in the current study. Each of these assumptions has to be validated for a particular polymer system under consideration. As we noted already, the chemical structure of real highly charged PEs might limit the dipole rotations to some extent, reducing thereby the fluctuation-mediated DD attraction and impeding the subsequent chain compaction.

From our theoretical considerations of a single PE chain with attractive DD interactions, section 3, follows that upon increase in salt amount weakly charged PE chains reduce their size, due to a weaker ES repulsion between the segments. The size of highly charged PEs with charge densities $\xi \gg 1$ reveals however a nonmonotonic dependence on the amount of added salt. In particular, in the limit of low salt concentrations $n_0 \lesssim 0.01$ M, the size of compact PE structures is reduced upon addition of salt; see Figure 4. On the contrary, for salt concentrations in the physiological range and higher up to 1 M, the compact PE globules start to swell upon addition of salt, due to stronger screening of attractive DD interactions. This globule swelling at high salts is in agreement with the general conclusions of ref 21 for the PE complexes in the regime dominated by attractive DD interactions.

4.2. Two PE Chains. In the second study, the complexation of two oppositely charged PE chains with their explicit counterions and salt ions has been studied by Langevin dynamics computer simulations.[26] For a single highly charged PE chain, it was calculated how the chain dimensions change and how the counterions accumulate on the chain as its charge density grows. Strong deviations from the Manning picture of counterion condensation were observed. For two PEs, the formation of helical-like aggregates and subsequent PE compaction into dense globules with interpenetrating PE chains was revealed, similarly to the results presented in ref 24 and shown in Figure 6 above. It was however suggested that the complexation mechanism of two oppositely charged PEs might be of entropic nature, in particular for strongly charged PEs.

Namely, at vanishing salinity, the complex formation was shown to be governed by PE−PE ES attraction at PE charge densities lower than $\sim 1.5\xi_M$, while for PEs with much higher charge densities the release of condensed counterions rather dominated the complex formation.[26] In this second regime, entropically driven counterions' release overcomes the unfavorable ES energy of complexation of two PEs. It was also shown that upon addition of 0.1−0.5 M of simple salt the free energy of the complex formation decreases for all chain linear charge densities. For weakly charged PEs, this hindered complexation originates from moderately lower ES complex formation energy because of screened ES interactions between the PE chains. For strongly charged PEs, on the other hand, the entropic gain of counterions evaporated from the PEs into solution is reduced dramatically, because the entropy difference driving the collapse in this limit scales like $\propto \ln(n(r)/n_0)$ and highly concentrated salt solutions offer smaller entropy preference for the counterions released.

It is hard to estimate the implications of this study on the data analyzed in Figure 7 for complexation of two PEs without any counterions in salt-free solution. The system of two PEs with small proximal mobile ions neutralizing the PE charge is indeed likely to be lower in energy than the system of two PEs with the charge compensated internally by another PE. The PE−PE complexation in this case might be triggered by the entropy increase by evaporated counterions.[52] For the two PEs without any explicit ions, the only driving force for the complexation is the ES attraction between them, and the impact of this attraction onto the chains' conformational properties was analyzed in section 3. Also, it is important to note that the complex formation in the system of two oppositely charged polyelectrolytes in simulations was observed at PE charge densities much lower than the counterion condensation thresh-

old. For instance, for the PE chains with 160 monomers in Figure 7, the collapse starts at only 0.1 of the critical Manning's PE linear charge density, when no counterions are condensed on the chain.

5. Conclusions

We have theoretically investigated the ES-driven coil−globule transition for a single highly charged PE chain with condensed counterions and for the mixture of two oppositely charged PEs.

In the first part, using the statistics of flexible polymers, we have studied the dimensions of coil and globular structures formed by a PE chain in the presence of attractive and repulsive interactions between the chain monomers. Below the Manning limit, the PE chain swells due to ES intermonomer repulsions. Above the $\xi \approx 1$ threshold, the dipoles are progressively formed on the chain due to counterion condensation and attractive average DD interactions between them trigger the PE collapse. The scaling relations for the size of compacting PEs obtained from the model of weakly perturbed Gaussian polymer differ for the case with and without excluded volume intermonomer interactions. The prediction for the complex size with excluded volume contribution reveals a good agreement with the results of molecular dynamics computer simulations of compaction of a single highly charged PE with explicit counterions.[23]

In the second part, we have analyzed the scaling relations for complexation of two oppositely charged PEs in weak and strong association regimes. Similarly to a single PE chain, the complexes of two PEs first swell at low ξ values and they enter the collapse regime as the chain linear charge density grows. Contrary to a single PE, however, where the collapse transition starts at $\xi \approx 1$ independently on the chain length, the complexation of two PEs is governed by attractive ES PE−PE association energy that scales in the coiled PE state as $\propto N^2$ with the chain length. Thus, longer PE chains can onset onto the collapse at interaction strengths up to 100 times lower than the Manning limit for a single chain. In the weak association regime, we utilize the model of ES blobs and show that PE−PE collapse transition can be understood in terms of fluctuation-induced ES interactions that facilitate ordering of charges and subsequently the complexation of ES blobs themselves. We suggest an explanation for why the globule size dependence observed in simulations and predicted theoretically for the two PEs is much weaker than that for a single PE chain with DD attractive interactions. In the strong PE−PE association regime, when a pronounced ion-crystal-like clustering of opposite charges in the PE complexes takes place, we suggest some scaling arguments for the globule size that exhibit even weaker ξ-dependence than the $R(\xi)$-scaling in the weak PE−PE interaction regime. This weak dependence can be attributed to a plateau in the $R_g(\xi)$ curve observed in the MD simulations[24] for very dense highly charged PE complexes at $\xi \gtrsim 20$.

Acknowledgment. I acknowledge many helpful discussions with R. G. Winkler, valuable comments of M. Castelnovo, Y. Kantor, M. Kardar, and H. Schiessel, insightful comments of the reviewers, as well as the financial support by the DFG through the Grant CH 707/2-2.

References and Notes

(1) Schiessel, H. *J. Phys.: Condens. Matter* **2003**, *15*, R699.
(2) Kunze, K. K.; Netz, R. R. *Phys. Rev. E* **2002**, *66*, 011918.
(3) Cherstvy, A. G.; Winkler, R. G. *J. Phys. Chem. B* **2005**, *109*, 2962.
(4) Cherstvy, A. G. *J. Phys. Chem. B* **2009**, *113*, 4242.
(5) Bloomfield, V. A. *Curr. Opin. Struct. Biol.* **1996**, *6*, 334.
(6) Takenaka, Y.; et al. *J. Chem. Phys.* **2005**, *123*, 014902.
(7) Cherstvy, A. G. *J. Phys.: Condens. Matter* **2005**, *17*, 1363.
(8) Oosawa, F. *Polyelectrolytes*; Dekker: New York, 1971.
(9) Manning, G. S. *Q. Rev. Biophys.* **1978**, *11*, 179.
(10) Manning, G. S. *J. Phys. Chem. B* **2007**, *111*, 8554.
(11) Schiessel, H.; Pincus, P. *Macromolecules* **1998**, *31*, 7953.
(12) Schiessel, H. *Macromolecules* **1999**, *32*, 5673.
(13) Muthukumar, M. *J. Chem. Phys.* **1996**, *104*, 691.
(14) Borue, V. Yu.; Erukhimovich, I. Ya. *Macromolecules* **1990**, *23*, 3625.
(15) Brilliantov, N. V.; Kuznetsov, D. V.; Klein, R. *Phys. Rev. Lett.* **1998**, *81*, 1433.
(16) Podgornik, R. *Phys. Rev. E* **2004**, *70*, 031801.
(17) Hansen, P. L.; et al. *Phys. Rev. E* **1999**, *60*, 1956.
(18) Kramarenko, E. Yu.; Erukhimovich, I. Ya.; Khokhlov, A. R. *Macromol. Theor. Simul.* **2002**, *11*, 463.
(19) Kuhn, P. S.; et al. *Physica A* **2004**, *337*, 481.
(20) Golestanian, R.; Kardar, M.; Liverpool, T. B. *Phys. Rev. Lett.* **1999**, *82*, 4456.
(21) Kumar, R.; Fredrickson, G. H. *J. Chem. Phys.* **2009**, *131*, 104901.
(22) Wang, Z.; Rubinstein, M. *Macromolecules* **2006**, *39*, 5897.
(23) Winkler, R. G.; Gold, M.; Reineker, P. *Phys. Rev. Lett.* **1998**, *80*, 3731.
(24) Winkler, R. G.; Steinhauser, M. O.; Reineker, P. *Phys. Rev. E* **2002**, *66*, 021802.
(25) von Ferber, C.; Loewen, H. *J. Chem. Phys.* **2003**, *118*, 10774.
(26) Ou, Z.; Muthukumar, M. *J. Chem. Phys.* **2006**, *124*, 154902.
(27) Winkler, R. G. *New J. Phys.* **2004**, *6*, 11.
(28) Muthukumar, M. *J. Chem. Phys.* **2004**, *120*, 9343.
(29) Loh, P.; et al. *Macromolecules* **2008**, *41*, 9352.
(30) Frank, S.; Winkler, R. G. *EPL* **2008**, *83*, 38004.
(31) Castelnovo, M.; Sens, P.; Joanny, J.-F. *Eur. Phys. J. E* **2000**, *1*, 115.
(32) Kandu, M.; Dobnikar, J.; Podgornik, R. *Soft Matter* **2009**, *5*, 868.
(33) Allahyarov, E.; Gompper, G.; Loewen, H. *J. Phys.: Condens. Matter* **2005**, *17*, S1827.
(34) Cherstvy, A. G. *J. Phys. Chem. B* **2007**, *111*, 7914.
(35) Israelachvili, J. N. *Intermolecular and Surface Forces*; Academic Press: 1992.
(36) Cherstvy, A. G.; Kornyshev, A. A. *J. Phys. Chem. B* **2005**, *109*, 13024.
(37) Rice, S. A.; Nagasawa, M.; Moravetz, H. *Polyelectrolyte solutions*; Academic Press: London, New York, 1961.
(38) Katchalsky, A.; Kunzle, O.; Kuhn, W. *J. Polym. Sci.* **1950**, *3*, 283.
(39) Lifson, S.; Katchalsky, A. *J. Polym. Sci.* **1953**, *XI*, 409.
(40) Liao, Q.; et al. *Macromolecules* **2006**, *39*, 1920.
(41) Jeon, J.; Dobrynin, A. V. *Macromolecules* **2007**, *40*, 7695.
(42) Higgs, P. G.; Joanny, J.-F. *J. Chem. Phys.* **1991**, *94*, 1543.
(43) Wittmer, J.; Johner, A.; Joanny, J.-F. *Europhys. Lett.* **1993**, *24*, 263.
(44) Everaers, R.; Johner, A.; Joanny, J.-F. *Europhys. Lett.* **1997**, *37*, 275.
(45) Yamakov, V.; et al. *Phys. Rev. Lett.* **2000**, *85*, 4305.
(46) Castelnovo, M.; Joanny, J.-F. *Macromolecules* **2002**, *35*, 4531.
(47) Kantor, Y.; Kardar, M. *Phys. Rev. E* **1995**, *53*, 835.
(48) Hayashi, Y.; Ullner, M.; Linse, P. *J. Chem. Phys.* **2002**, *116*, 6836.
(49) Hayashi, Y.; Ullner, M.; Linse, P. *J. Phys. Chem. B* **2003**, *107*, 8198.
(50) Guskova, O. A.; et al. *Polym. Sci., Ser. A* **2006**, *48*, 763.
(51) Oskolkov, N. N.; Potemkin, I. I. *Macromolecules* **2007**, *40*, 8423.
(52) Note however that if the concentration of counterions near a negatively charged rod $\Psi(r) < 0$ follows the distribution, $n(r) = n_0 e^{-\Psi(r)}$, the entropy gain to remove a positive ion from distance r from the cylinder to infinity, $T\Delta S(r) = -k_B T\Psi(r) > 0$, is exactly balanced by the loss of the ion−rod ES interaction energy.
(53) Kundagrami, A.; Muthukumar, M. *Macromolecules* **2010**, *43*, 2574.

JP910960R